

Modifications by QCD transition and e^+e^- annihilation on analytic spectrum of relic gravitational waves in accelerating universe

S. Wang¹, Y. Zhang¹[*], T.Y. Xia¹, and H.X. Miao^{1,2}

¹Astrophysics Center, University of Science and Technology of China, Hefei, Anhui, 230026, China

²AIGO, University of Western Australia, WA 6009, Australia

Abstract

As predicted by quantum chromodynamics(QCD), around $T \sim 190$ MeV in the early universe, the QCD transition occurs during which the quarks are combined into the massive hadrons. This process reduces the effective relativistic degree of freedom, and causes a change in the expansion behavior of the universe. Similarly, the e^+e^- annihilation occurred around $T \sim 0.5$ MeV has the same kind of effect. Besides, the dark energy also drives the present stage accelerating expansion. We study these combined effects on the relic gravitational waves (RGWs). In our treatment, the QCD transition and the e^+e^- annihilation, each is respectively represented by a short period of expansion inserted into the radiation era. Incorporating these effects, the equation of RGWs is analytically solved for a spatially flat universe, evolving from the inflation up to the current acceleration, and the spectrum of RGWs is obtained, covering the whole range of frequency $> 10^{-19}$ Hz. It is found that the QCD transition causes a reduction of the amplitude of RGWs by $\sim 20\%$ in the range $> 10^{-9}$ Hz, and the e^+e^- annihilation causes a reduction $\sim 10\%$ in the range $> 10^{-12}$ Hz. In the presence of the dark energy, the combination of the QCD transition and the e^+e^- annihilation, causes a larger reduction of the amplitude by $\sim 30\%$ for the range $> 10^{-9}$ Hz, which covers the bands of operation of LIGO and LISA. By analysis, it is shown that RGWs will be difficult to detect by the present LIGO, but can be tested by LISA for certain inflationary models.

PACS numbers: 04.30.-w, 98.80.-k, 04.62.+v

1. Introduction

The existence of a stochastic background of relic gravitational waves (RGWs) is generally predicted in inflationary models [1, 2, 3]. Since the relic gravitons decoupled much earlier than the cosmic microwave background (CMB) photons, the detections of RGWs would open a new window to the very early universe. Unlike gravitational radiations from finite stellar objects, RGWs exist everywhere and anytime, and have a wide spreading spectrum, serving as one of the major scientific goals of the laser interferometers gravity-wave detections, including the current LIGO [4], VIRGO [5], GEO600 [6], TAMA [7], AIGO [8], and the future LISA [9], ASTROD [10], BBO [11], and DECIGO [12]. Moreover, along with the density perturbations, RGWs also contribute to the CMB anisotropies and polarizations [13, 14, 15, 16, 17]. For instance, the B-polarization of CMB on very large scales can only be generated by RGWs. Through the detections of CMB polarizations one may have a chance to obtain the direct evidence of GWs for the first time [18, 19, 20, 21, 22]. Therefore, the precise information of RGWs is much desired.

The spectrum of RGWs depends on the following factors. First, it depends sensitively on the specific inflationary models [1, 3, 23]. After being generated, it will be altered by the subsequent stages of expansion of the universe, among which notably is the currently accelerating expansion of the universe [3, 24]. Finally, it would be further modified by other physical processes occurred in the early universe. For example, the neutrino free-streaming [25] has been shown to affect the spectrum of RGWs in the very low frequency range ($10^{-16} \sim 10^{-10}$) Hz [26]. Although this would modify the contribution to CMB polarizations, but would not affect the detections of LIGO [4] and LISA [9] that operate effectively at higher frequencies, ($10^1 \sim 10^3$) Hz and ($10^{-7} \sim 10^0$) Hz, respectively. Other important physical processes include the QCD transition around a temperature $T \sim 190$ MeV [27, 28], and the e^+e^- annihilation around $T \sim 0.5$ MeV. These two processes will be studied in this work. Leaving aside the detail of the QCD transition, which is notoriously complicated and still under study, we are concerned with only the thermodynamic property that the transition brings to the system, i.e., a significant drop in the relativistic degrees of freedom. Consequently, the constituent components in the stress tensor $T_{\mu\nu}$ also change in the Friedmann's equation. Thereby the expansion of the Universe in terms of the scale factor $a(\tau)$ will subsequently change, and the spectrum of RGWs would be modified. The e^+e^- annihilation has the similar effect. Schwarz [29] studied the QCD transition and the e^+e^- annihilation and estimated the reduction of the energy density spectrum of RGWs. Watanabe and Komatsu [30] investigated these effects with more details, and gave a numerical solution of the energy density spectrum of RGWs. In these works, the important effect of the accelerating expansion of the present universe [3] has not been included, neither the effects of inflation and reheating. Moreover, to show the prospects of detecting RGWs at the laser interferometers gravity-wave detection, an explicit demonstration of the current spectrum of RGWs itself and its direct comparison with the sensitivity curve of gravity-wave detection are also needed.

In this paper, by extending our previous analytical calculation of the spectrum of RGWs, we explore the consequences caused by the QCD transition and the e^+e^- annihilation, and, at the same time, take into account of the accelerating expansion driven by the dark energy [3]. Beside the energy density spectrum $\Omega_g(\nu)$, we demonstrate explicitly the spectrum $h(\nu, \tau_H)$ of RGWs itself, and compare it directly with the sensitivity of the ongoing and forthcoming GW detectors, such as LIGO, LISA, etc [4–9]. Aiming at giving

a comprehensive compilation, by using the set of parameters β , β_s , n , v , γ and r , respectively, such important cosmological elements have been explicitly parameterized, as the inflation, the reheating, the QCD transition, the e^+e^- annihilation, the dark energy and the tensor/scalar ratio. This will considerably facilitate further studies on the RGWs and the relevant physical processes. For instance, it can be easily used in the calculation of CMB anisotropies and polarizations generated by RGWs [16, 21].

The organization of this paper is as follows. In section 2, from the inflation up to the acceleration, the scale factor $a(\tau)$ is specified by the continuity conditions for the subsequential stages of expansion. The periods of the QCD transition and the e^+e^- annihilation are also modelled as having a scale factor $a(\tau)$ of power-law form, which is inserted into the radiation era. In section 3, the analytical solution of RGWs in terms of Bessel's functions is determined with the coefficients being fixed by continuity condition joining two consecutive expansion stages. The impact of the dark energy on the expansion is emphasized. In section 4, we present the resulting spectra of RGWs and discuss the modifications caused by the QCD transition, the e^+e^- annihilation, and other effects. Appendix A supplies the details of our treatment of the period of QCD transition and e^+e^- annihilation by modelling the corresponding scale factor. Appendix B gives an interpretation of the modifications on RGWs due to the QCD transition. In this paper the unit with $c = \hbar = k_B = 1$ is used.

2. Expansion history of the universe

From the inflationary up to the currently accelerating stage, the expansion of the universe can be described by the spatially flat ($\Omega_\Lambda + \Omega_m + \Omega_r = 1$) Robertson-Walker spacetime with a metric

$$ds^2 = a^2(\tau)[-d\tau^2 + \delta_{ij}dx^i dx^j], \quad (1)$$

where τ is the conformal time. The scale factor $a(\tau)$ for the successive stages can be approximately described by the following forms [31]:

The inflationary stage:

$$a(\tau) = l_0 |\tau|^{1+\beta}, \quad -\infty < \tau \leq \tau_1, \quad (2)$$

where $1 + \beta < 0$, and $\tau_1 < 0$. This generic form of scale factor is a simple modelling of inflationary expansion, and the index β is a parameter. The special case of $\beta = -2$ is the de Sitter expansion of inflation. If the inflationary expansion is driven by a scalar field, then the index β is related to the so-called slow-roll parameters, η and ϵ [32], as $\beta = -2 + (\eta - 3\epsilon)$. In this class of scalar inflationary models one usually has $\beta \leq -2$. Besides, the observational results of WMAP also indicate that β should be slightly smaller than -2 [18]. But, for demonstration purpose, we allow the parameter β to take values > -2 to examine the possibility of detection by GWS detectors.

The reheating stage:

$$a(\tau) = a_z |\tau - \tau_p|^{1+\beta_s}, \quad \tau_1 \leq \tau \leq \tau_s, \quad (3)$$

where τ_s is the beginning of radiation era and $\tau_p < \tau_1$. We will mostly take the model parameter $\beta_s = -0.3$, though other values are also taken to demonstrate the effect of various reheating models.

The radiation-dominant stage:

The QCD transition occurs around $T \sim 190$ MeV for a period, and the process of e^+e^- annihilation into photons starts around $T \sim 0.5$ MeV and ends up around $T \sim 0.1$ MeV [30]. These two periods should be included into the radiation stage. Before the QCD transition, one has

$$a(\tau) = a_e(\tau - \tau_e), \quad \tau_s \leq \tau \leq \tau_q; \quad (4)$$

where τ_q is the beginning of the QCD transition and $\tau_e < \tau_s$. During the QCD transition, $a(\tau)$ is modelled by

$$a(\tau) = a_n(\tau - \tau_n)^{1+n}, \quad \tau_q \leq \tau \leq \tau_x, \quad (5)$$

where τ_x is the ending of the QCD transition and $\tau_n < \tau_q$. The power index n in Eq.(5) is a model parameter describing the QCD transition. We have found that the spectrum of RGWs does not vary considerably for the values of n in the interval $(0.7 \sim 4.6)$. For concreteness we take $n = 1.634$ in calculations. (For more details, see Appendix A). The expansion rate $a'(\tau)$ around $T \sim 190$ MeV is plotted in Fig.1, showing a jump-up caused by the QCD transition. After the QCD transition and before the e^+e^- annihilation, one has

$$a(\tau) = a_f(\tau - \tau_f), \quad \tau_x \leq \tau \leq \tau_y, \quad (6)$$

where τ_y is the beginning of the e^+e^- annihilation and $\tau_f < \tau_x$. The two slopes a_e in Eq.(4) and a_f in Eq.(6) are related as $a_f \simeq 1.2a_e$ by considerations of the details of the QCD transition (See Appendix A). Similarly, the period of e^+e^- annihilation is modelled by

$$a(\tau) = a_v(\tau - \tau_v)^{1+v}, \quad \tau_y \leq \tau \leq \tau_z, \quad (7)$$

where τ_z is the ending of the e^+e^- annihilation and $\tau_v < \tau_y$. The power index v in Eq.(7), as a model parameter, can be taken as $v = 0.063$ (see Appendix A). After the e^+e^- annihilation, one has

$$a(\tau) = a_g(\tau - \tau_g), \quad \tau_z \leq \tau \leq \tau_2, \quad (8)$$

where $\tau_g < \tau_z$, and τ_2 is the beginning of the matter era, which can be taken at a redshift $z \simeq 3454$ [18]. The two slopes a_f in Eq.(6) and a_g in Eq.(8) satisfy the relation $a_g \simeq 1.1a_f$ (See Appendix A).

The matter-dominant stage:

$$a(\tau) = a_m(\tau - \tau_m)^2, \quad \tau_2 \leq \tau \leq \tau_E, \quad (9)$$

where $\tau_m < \tau_2$ and τ_E is the beginning of the acceleration era.

The accelerating stage:

$$a(\tau) = l_H |\tau - \tau_a|^{-\gamma}, \quad \tau_E \leq \tau \leq \tau_H, \quad (10)$$

where τ_H is the present time and $\tau_H < \tau_a$. The index γ in Eq.(10) depends on the dark energy Ω_Λ . By fitting with the numerical solution of the Friedmann equation [3, 26],

$$\left(\frac{a'}{a^2}\right)^2 = \frac{8\pi G}{3}(\rho_\Lambda + \rho_m + \rho_r), \quad (11)$$

where $a' \equiv da/d\tau$, one can take $\gamma \simeq 1.05$ for $\Omega_\Lambda = 0.7$, and $\gamma \simeq 1.044$ for $\Omega_\Lambda = 0.75$. The redshift of the start of this stage depends on the specific models of the dark energy. For instance, in the cosmological

constant model with $\Omega_\Lambda = 0.72$ and $\Omega_m = 0.28$, it starts at $z \simeq 0.37$, and, in the quantum effective Yang-Mills condensate dark energy model, it starts at $z \simeq 0.5$ [33].

In the above specifications of $a(\tau)$, there are nine instances of time, $\tau_1, \tau_s, \tau_q, \tau_x, \tau_y, \tau_z, \tau_2, \tau_E$, and τ_H , which separate the different stages. Eight of them are determined by how much $a(\tau)$ increases over each stage based on the cosmological considerations. We take the following specifications: $\zeta_1 \equiv \frac{a(\tau_s)}{a(\tau_1)} = 300$ for the reheating stage, $\zeta_s \equiv \frac{a(\tau_q)}{a(\tau_s)} = 2.895 \times 10^{16}$ for the first radiation stage, $\zeta_q \equiv \frac{a(\tau_x)}{a(\tau_q)} = 1.34$ for the second radiation stage, $\zeta_x \equiv \frac{a(\tau_y)}{a(\tau_x)} = 283.582$ for the third radiation stage, $\zeta_y \equiv \frac{a(\tau_z)}{a(\tau_y)} = 5$ for the fourth radiation stage, $\zeta_z \equiv \frac{a(\tau_2)}{a(\tau_z)} = 1.818 \times 10^4$ for the fifth radiation stage (see Appendix A), $\zeta_2 \equiv \frac{a(\tau_E)}{a(\tau_2)} = 3454\zeta_E^{-1}$ for the matter stage, and $\zeta_E \equiv \frac{a(\tau_H)}{a(\tau_E)} = (\frac{\Omega_\Lambda}{\Omega_m})^{1/3}$ for the present accelerating stage [3, 26]. The remaining time instance is fixed by an overall normalization

$$|\tau_H - \tau_a| = 1. \quad (12)$$

There are also 22 constants in the expressions of $a(\tau)$, among which β, β_s, n, v and γ are imposed as the model parameters describing the inflation, the reheating, the QCD transition, the e^+e^- annihilation and the acceleration, respectively. Based on the definition of the expansion rate $H_0 = \frac{a'}{a^2}|_{\tau_H}$ of the present universe, one has $l_H = \gamma/H_0$. Making use of the continuity conditions of $a(\tau)$ and of $a(\tau)'$ at the eight given joining points $\tau_1, \tau_s, \tau_q, \tau_x, \tau_y, \tau_z, \tau_2, \tau_E$, and τ_H , all parameters are fixed as the following:

$$\begin{aligned} \tau_a - \tau_E &= \zeta_E^{\frac{1}{\gamma}}, \\ \tau_E - \tau_m &= \frac{2}{\gamma} \zeta_E^{\frac{1}{\gamma}}, \\ \tau_2 - \tau_m &= \frac{2}{\gamma} \zeta_2^{-\frac{1}{2}} \zeta_E^{\frac{1}{\gamma}}, \\ \tau_2 - \tau_g &= \frac{1}{\gamma} \zeta_2^{-\frac{1}{2}} \zeta_E^{\frac{1}{\gamma}}, \\ \tau_z - \tau_g &= \frac{1}{\gamma} \zeta_z^{-1} \zeta_2^{-\frac{1}{2}} \zeta_E^{\frac{1}{\gamma}}, \\ \tau_z - \tau_v &= \frac{1}{\gamma} (1+v) \zeta_z^{-1} \zeta_2^{-\frac{1}{2}} \zeta_E^{\frac{1}{\gamma}}, \\ \tau_y - \tau_v &= \frac{1}{\gamma} (1+v) \zeta_y^{-\frac{1}{1+v}} \zeta_z^{-1} \zeta_2^{-\frac{1}{2}} \zeta_E^{\frac{1}{\gamma}}, \\ \tau_y - \tau_f &= \frac{1}{\gamma} \zeta_y^{-\frac{1}{1+v}} \zeta_z^{-1} \zeta_2^{-\frac{1}{2}} \zeta_E^{\frac{1}{\gamma}}, \\ \tau_x - \tau_f &= \frac{1}{\gamma} \zeta_x^{-1} \zeta_y^{-\frac{1}{1+v}} \zeta_z^{-1} \zeta_2^{-\frac{1}{2}} \zeta_E^{\frac{1}{\gamma}}, \\ \tau_x - \tau_n &= \frac{1}{\gamma} (1+n) \zeta_x^{-1} \zeta_y^{-\frac{1}{1+v}} \zeta_z^{-1} \zeta_2^{-\frac{1}{2}} \zeta_E^{\frac{1}{\gamma}}, \\ \tau_q - \tau_n &= \frac{1}{\gamma} (1+n) \zeta_q^{-\frac{1}{1+n}} \zeta_x^{-1} \zeta_y^{-\frac{1}{1+v}} \zeta_z^{-1} \zeta_2^{-\frac{1}{2}} \zeta_E^{\frac{1}{\gamma}}, \\ \tau_q - \tau_e &= \frac{1}{\gamma} \zeta_q^{-\frac{1}{1+n}} \zeta_x^{-1} \zeta_y^{-\frac{1}{1+v}} \zeta_z^{-1} \zeta_2^{-\frac{1}{2}} \zeta_E^{\frac{1}{\gamma}}, \\ \tau_s - \tau_e &= \frac{1}{\gamma} \zeta_s^{-1} \zeta_q^{-\frac{1}{1+n}} \zeta_x^{-1} \zeta_y^{-\frac{1}{1+v}} \zeta_z^{-1} \zeta_2^{-\frac{1}{2}} \zeta_E^{\frac{1}{\gamma}}, \\ \tau_s - \tau_p &= \frac{1}{\gamma} |1 + \beta_s| \zeta_s^{-1} \zeta_q^{-\frac{1}{1+n}} \zeta_x^{-1} \zeta_y^{-\frac{1}{1+v}} \zeta_z^{-1} \zeta_2^{-\frac{1}{2}} \zeta_E^{\frac{1}{\gamma}}, \\ \tau_1 - \tau_p &= \frac{1}{\gamma} |1 + \beta_s| \zeta_1^{-\frac{1}{1+\beta_s}} \zeta_s^{-1} \zeta_q^{-\frac{1}{1+n}} \zeta_x^{-1} \zeta_y^{-\frac{1}{1+v}} \zeta_z^{-1} \zeta_2^{-\frac{1}{2}} \zeta_E^{\frac{1}{\gamma}}, \end{aligned}$$

$$\tau_1 = \frac{1}{\gamma} (1 + \beta) \zeta_1^{-\frac{1}{1+\beta_s}} \zeta_s^{-1} \zeta_q^{-\frac{1}{1+n}} \zeta_x^{-1} \zeta_y^{-\frac{1}{1+v}} \zeta_z^{-1} \zeta_2^{-\frac{1}{2}} \zeta_E^{\frac{1}{\gamma}}, \quad (13)$$

and

$$\begin{aligned} a_m &= l_H \frac{\gamma^2}{4} \zeta_E^{-(1+\frac{2}{\gamma})}, \\ a_g &= l_H \gamma \zeta_2^{-\frac{1}{2}} \zeta_E^{-(1+\frac{1}{\gamma})}, \\ a_v &= l_H \gamma^{1+v} |1+v|^{-(1+v)} \zeta_z^v \zeta_2^{\frac{v-1}{2}} \zeta_E^{-(1+\frac{1+v}{\gamma})}, \\ a_f &= l_H \gamma \frac{10}{11} \zeta_2^{-\frac{1}{2}} \zeta_E^{-(1+\frac{1}{\gamma})}, \\ a_n &= l_H \frac{10}{11} \gamma^{1+n} |1+n|^{-(1+n)} \zeta_x^n \zeta_y^{\frac{n}{1+v}} \zeta_z^n \zeta_2^{\frac{n-1}{2}} \zeta_E^{-(1+\frac{1+n}{\gamma})}, \\ a_e &= l_H \gamma \frac{25}{33} \zeta_2^{-\frac{1}{2}} \zeta_E^{-(1+\frac{1}{\gamma})}, \\ a_z &= l_H \frac{25}{33} \gamma^{1+\beta_s} |1+\beta_s|^{-(1+\beta_s)} \zeta_s^{\beta_s} \zeta_q^{\frac{\beta_s}{1+n}} \zeta_x^{\beta_s} \zeta_y^{\frac{\beta_s}{1+v}} \zeta_z^{\beta_s} \zeta_2^{\frac{\beta_s-1}{2}} \zeta_E^{-(1+\frac{1+\beta_s}{\gamma})}, \\ l_0 &= l_H \frac{25}{33} \gamma^{1+\beta} |1+\beta|^{-(1+\beta)} \zeta_1^{\frac{\beta-\beta_s}{1+\beta_s}} \zeta_s^\beta \zeta_q^{\frac{\beta}{1+n}} \zeta_x^\beta \zeta_y^{\frac{\beta}{1+v}} \zeta_z^\beta \zeta_2^{\frac{\beta-1}{2}} \zeta_E^{-(1+\frac{1+\beta}{\gamma})}. \end{aligned} \quad (14)$$

In the expanding universe, the physical wavelength is related to the comoving wavenumber k by

$$\lambda \equiv \frac{2\pi a(\tau)}{k}, \quad (15)$$

and the wavenumber k_H corresponding to the present Hubble radius is

$$k_H = \frac{2\pi a(\tau_H)}{1/H_0} = 2\pi\gamma. \quad (16)$$

There is another wavenumber involved

$$k_E \equiv \frac{2\pi a(\tau_E)}{1/H_0} = \frac{k_H}{1+z_E}, \quad (17)$$

whose corresponding wavelength at the time τ_E is the Hubble radius $1/H_0$. In the present universe the physical frequency corresponding to a wavenumber k is given by

$$\nu = \frac{1}{\lambda} = \frac{k}{2\pi a(\tau_H)} = \frac{H_0}{2\pi\gamma} k. \quad (18)$$

3. Analytical solution of RGWs

In the presence of the gravitational waves, the perturbed metric is

$$ds^2 = a^2(\tau)[-d\tau^2 + (\delta_{ij} + h_{ij})dx^i dx^j], \quad (19)$$

where the tensorial perturbation h_{ij} is a 3×3 matrix and is taken to be transverse and traceless

$$h^i_i = 0, \quad h_{ij,j} = 0. \quad (20)$$

The wave equation of RGWs is

$$\partial_\nu (\sqrt{-g} \partial^\nu h_{\mu\nu}) = 0 \quad (21)$$

We decompose h_{ij} into the Fourier modes of the comoving wave number k and into the polarization state σ as

$$h_{ij}(\tau, \mathbf{x}) = \sum_{\sigma} \int \frac{d^3k}{(2\pi)^3} \epsilon_{ij}^{\sigma} h_k^{(\sigma)}(\tau) e^{i\mathbf{k}\cdot\mathbf{x}}, \quad (22)$$

where $h_{-k}^{(\sigma)*}(\tau) = h_k^{(\sigma)}(\tau)$ ensuring that h_{ij} be real, ϵ_{ij}^{σ} is the polarization tensor, and σ denotes the polarization states $\times, +$. Here h_{ij} is treated as a classical field. In terms of the mode $h_k^{(\sigma)}$, Eq.(21) reduces to

$$h_k^{(\sigma)''}(\tau) + 2\frac{a'(\tau)}{a(\tau)}h_k^{(\sigma)'}(\tau) + k^2h_k^{(\sigma)}(\tau) = 0. \quad (23)$$

By assumption, for each polarization, $\times, +$, the wave equation is the same and has the same statistical properties, so that the super index (σ) can be dropped from $h_k^{(\sigma)}$ from now on. Since for all the stages of expansion the scale factor is of a power-law form

$$a(\tau) \propto \tau^{\alpha} \quad (24)$$

the solution to Eq.(23) is a linear combination of Bessel function J_{ν} and Neumann function N_{ν}

$$h_k(\tau) = \tau^{\frac{1}{2}-\alpha} \left[a_1 J_{\alpha-\frac{1}{2}}(k\tau) + a_2 N_{\alpha-\frac{1}{2}}(k\tau) \right], \quad (25)$$

where the constants a_1 and a_2 are completely determined by the continuity of h_k and of h_k' at the joining points $\tau_1, \tau_s, \tau_q, \tau_x, \tau_y, \tau_z, \tau_2$, and τ_E .

In particular, we write down explicitly the solution for the inflationary stage since it give the initial condition for the spectrum of RGWs,

$$h_k(\tau) = A_0 l_0^{-1} |\tau|^{-\frac{1}{2}-\beta} \left[A_1 J_{\frac{1}{2}+\beta}(x) + A_2 J_{-(\frac{1}{2}+\beta)}(x) \right], \quad -\infty < \tau \leq \tau_1 \quad (26)$$

where $x \equiv k\tau$ and

$$A_1 = -\frac{i}{\cos \beta \pi} \sqrt{\frac{\pi}{2}} e^{i\pi\beta/2}, \quad A_2 = \frac{1}{\cos \beta \pi} \sqrt{\frac{\pi}{2}} e^{-i\pi\beta/2}, \quad (27)$$

are taken [34], so that the so-called *adiabatic vacuum* is achieved: $\lim_{k \rightarrow \infty} h_k(\tau) \propto e^{-ik\tau}$ in the high frequency limit [35]. Moreover, the constant A_0 in Eq.(26) is independent of k , whose value is determined by the initial amplitude of the spectrum. For $k\tau \ll 1$ the k -dependence of $h_k(\tau)$ is given by

$$h_k(\tau) \propto J_{\frac{1}{2}+\beta}(x) \propto k^{\frac{1}{2}+\beta}. \quad (28)$$

As will be seen later, this choice will lead to the required scale-invariant initial spectrum in Eq.(32).

It should be mentioned that around the temperature $T \sim 2$ Mev neutrinos decoupled from electrons and photons and started free-streaming in space. This will give rise to an anisotropic part of the energy-momentum tensor as a source of the equation of RGWs. The previous works have shown that the neutrino free-streaming in combination with the dark energy would cause a reduction of the amplitude of RGWs by $\sim 20\%$ in the low frequency range ($10^{-16} \sim 10^{-10}$) Hz [25, 26, 30]. Although this modified RGWs will contribute to the CMB anisotropies and polarizations on very large scales, the frequency range is outside the frequency bands of LIGO and LISA. On the other hand, as will be seen, the impact on RGWs by the QCD transition is in the high frequency range $\nu > 10^{-9}$ Hz. Since these two frequency ranges are not overlapped, for simplicity of computing we will not include the neutrino free-streaming here

In our previous study [26], we have examined the issue of how the RGWs would be, if our current universe were matter-dominated. The amplitudes of RGWs in the Λ CDM (accelerating) and in the CDM universe were compared, and the ratio was found to be $h_k(\tau_H)_{\Lambda\text{CDM}}/h_k(\tau_H)_{\text{CDM}} \sim 1.3$. Here a similar examination is extended to the case including the QCD transition and the e^+e^- annihilation. To be specific, we assume that both universes have the same initial $a(\tau_2)$ and $a'(\tau_2)$ at the time τ_2 with $z \simeq 3454$, when $\rho_\Lambda \ll \rho_m = \rho_r$. By numerically solving the Friedmann equation in both models, we plot the scale factor $a(t)$ in Fig.2, showing that the ratio of scale factors at present is $a(\tau_H)_{\Lambda\text{CDM}}/a(\tau_H)_{\text{CDM}} \simeq 1.8$. As is known [1, 3], for wavelengths shorter than the horizon the modes decay as $h_k(\tau) \propto 1/a(\tau)$, so the CDM model would predict an amplitude of RGWs higher than the Λ CDM model. This is indeed confirmed by our calculation including the QCD transition and the e^+e^- annihilation, and the ratio is

$$h_k(\tau_H)_{\text{CDM}}/h_k(\tau_H)_{\Lambda\text{CDM}} \sim 1.8. \quad (29)$$

Moreover, there are some subtleties with the matter-dominant model, regarding to interpreting the current observations. As it stands, the actual universe is Λ CDM, so the observed Hubble constant is properly interpreted as the current expansion rate in the accelerating model, $H_0 = (a'/a^2)_{\tau_H}$. The virtual matter-dominant universe would have a smaller rate $(a'/a^2)_{\tau_H} \simeq 0.4H_0$. If the observed Hubble constant H_0 were regarded as the expansion rate of the virtual matter-dominant universe [30], one would come up with an amplitude of $h_k(\tau_H)$ lower by an extra factor ~ 1.8 than it should be.

4. Spectrum of relic gravitational waves

The spectrum of RGWs $h(k, \tau)$ at a time τ is defined by the following equation [31]:

$$\int_0^\infty h^2(k, \tau) \frac{dk}{k} \equiv \langle 0 | h^{ij}(\mathbf{x}, \tau) h_{ij}(\mathbf{x}, \tau) | 0 \rangle, \quad (30)$$

where the right-hand side is the expectation value of the $h^{ij}h_{ij}$. Calculation yields the spectrum at present

$$h(k, \tau_H) = \frac{2}{\pi} k^{3/2} |h_k(\tau_H)|, \quad (31)$$

where the factor 2 counts for the two independent polarizations.

One of the most important properties of the inflation is that the initial spectrum of RGWs at the time τ_i of the horizon-crossing during the inflation is nearly scale-invariant [31]:

$$h(k, \tau_i) = A \left(\frac{k}{k_H} \right)^{2+\beta}, \quad (32)$$

where $2 + \beta \simeq 0$, and A is a constant to be fixed by the observed CMB anisotropies in practice. The First Year WMAP gives the scalar spectral index $n_s = 0.99 \pm 0.04$, the Three Year WMAP gives $n_s = 0.951_{-0.019}^{+0.015}$ [18], while in combination with constraints from SDSS, SNIa, and the galaxy clustering, it would give $n_s = 0.965 \pm 0.012$ (68% CL) [20]. The five-year WMAP data give $n_s = 0.963_{-0.015}^{+0.014}$ [36], and the WMAP data combined with Baryon Acoustic Oscillations and Type Ia supernovae give $n_s = 0.960_{-0.013}^{+0.014}$ (95% CL) [37]. From the relation $n_s = 2\beta + 5$ [1, 3], the inflation index $\beta = -2.02$ for $n_s = 0.951$. As mentioned earlier we will allow the parameter β to take values > -2 to demonstrate the RGWs spectrum

Note that the constant A is directly proportional to A_0 in Eq.(26). Since the observed CMB anisotropies [18] is $\Delta T/T \simeq 0.37 \times 10^{-5}$ at $l \sim 10$, which corresponds to anisotropies on scales of the Hubble radius $1/H_0$, so, as in Refs.[26], we take the normalization of the spectrum

$$h(k_E, \tau_H) = 0.37 \times 10^{-5} r^{\frac{1}{2}}, \quad (33)$$

where k_E is defined in Eq.(17), its corresponding physical frequency being $\nu_E = k_E/2\pi a(\tau_H) = H_0/(1+z_E) \sim 1 \times 10^{-18}$ Hz. The tensor/scalar ratio r can be related to the slow roll parameter ϵ in the scalar inflationary model as $r = 16\epsilon$ [32]. However, the value of r is model-dependent, and frequency-dependent [16, 17]. This has long been known to be a notoriously thorny issue [38]. In our treatment, for simplicity, r is only taken as a constant parameter for normalization of RGWs. Currently, only observational constraints on r have been given. The Three Year WMAP constraint is $r < 2.2$ (95% CL) evaluated at $k = 0.002 \text{ Mpc}^{-1}$, and the full WMAP constraint is $r < 0.55$ (95% CL) [21]. The combination from such observations, as of SDSS, 3-year WMAP, supernovae SN, and galaxy clustering, gives an upper limit $r < 0.22$ (95% CL) [20]. The five-year WMAP gives a limit $r < 0.43$ (95%) for power-law models [36], and the WMAP data combined with Baryon Acoustic Oscillations and Type Ia supernovae give $r < 0.20$ (95% CL) [37]. For concreteness, we take $r = 0.22$.

The spectral energy density $\Omega_g(k)$ of the RGWs is given by

$$\Omega_g(k) = \frac{\pi^2}{3} h^2(k, \tau_H) \left(\frac{k}{k_H} \right)^2, \quad (34)$$

which follows from the definition of the total energy density of RGWs [31]

$$\Omega_{GW} \equiv \frac{\rho_g}{\rho_c} = \int_{k_{low}}^{k_{upper}} \Omega_g(k) \frac{dk}{k}, \quad (35)$$

where $\rho_g = \frac{1}{32\pi G} h_{ij,0} h_{,0}^{ij}$ is the energy density of RGWs, and $\rho_c = 3H_0^2/8\pi G$ is the critical energy density. The integration in Eq.(35) has the lower and upper limits, k_{low} and k_{upper} , as the cutoffs of the wavenumber. The corresponding frequencies are $\nu_{low} \simeq 2 \times 10^{-18}$ Hz and $\nu_{upper} \simeq 10^{10}$ Hz. Detailed analyses of these limits are given in Ref.[26]. In past, in the absence of direct detection of RGWs, the constraint on RGWs through the energy density Ω_{GW} has been commonly used; especially, a bound from the Big Bang nucleosynthesis (BBN) [39]

$$\Omega_{GW} h_0^2 < 8.9 \times 10^{-6} \quad (36)$$

has been frequently employed in practice, where $h_0 \sim 0.7$ being the Hubble parameter [18].

In the following we give the resulting spectra $h(k, \tau_H)$ and $\Omega_g(k)$ of RGWs, demonstrate their explicit dependence upon the model parameters β , β_s , γ , and the modifications by the QCD transition and e^+e^- annihilation. Also we will compare it with the sensitivity of detections, such as LIGO and LISA.

Figure 3 gives the spectrum $h(\nu, \tau_H)$ for three values of the inflationary index $\beta = -1.8, -1.9, \text{ and } -2.02$, respectively, where the fixed $r = 0.22$, $\Omega_\Lambda = 0.75$, $\beta_s = -0.3$, $n = 1.634$, and $v = 0.063$ are taken. It is seen that $h(\nu, \tau_H)$ is very sensitive to β . A smaller β will generate lower amplitude of RGWs for all frequencies.

Figure 4 shows the influence of reheating stage on RGWs. The spectrum is given for three different values of $\beta_s = 0.5, 0,$ and -0.3 . It is seen that the reheating process will affect RGWs only in very high frequency range $\nu > 10^7$ Hz. This covers the frequency range of some very high frequency gravity wave detection systems, such as the Gaussian laser beam detector aiming at the frequency $\nu \sim 10^{10}$ Hz [40], or the circular waveguide detector aiming at $\nu > 10^5$ Hz [41]. We remark that the portion of predicted spectrum for the frequency range $\nu > 10^{10}$ Hz may be not reliable. This is because the energy scale of the conventional inflationary models are usually less than 10^{16} GeV [26], which will give a cutoff of frequency around $\nu \sim 10^{10}$ Hz.

Presented in Fig.5 is the modification of the spectrum $h(\nu, \tau_H)$ by the QCD transition. There is a critical frequency $\nu_Q \simeq 10^{-9}$ Hz, below which the spectrum is the same for both models with or without the QCD transition. But, in the high frequency range $\nu > \nu_Q$ Hz, the amplitude of $h(\nu, \tau_H)$ is reduced by $\sim 20\%$ in comparison with the model without QCD transition.

$$h_k(\tau_H)_{no\ QCD}/h_k(\tau_H)_{QCD} \simeq 1.2 \quad \text{for } \nu > \nu_Q. \quad (37)$$

Note that the frequency range of this reduction on RGWs covers those of the major laser interferometers GW detectors, such as LIGO and VIRGO operating effectively in the frequency bands around $\sim 10^2$ Hz, and LISA around $\sim 10^{-3}$ Hz, respectively. So the modifications on RGWs due to the QCD transition are relevant to these major detections. In Appendix B we will give an interpretation to the origin of this critical frequency $\nu_Q = 10^{-9}$ Hz and of the reduction in amplitude by $\sim 20\%$ for $\nu > \nu_q$ Hz.

Fig.6 gives the spectrum $h(\nu, \tau_H)$ modified by the e^+e^- annihilation, which has a similar reduction effect. The lower frequency portion $\nu < 10^{-12}$ Hz of the spectrum is not affected by the e^+e^- annihilation. However, in the high frequency range $\nu > 10^{-12}$ Hz, the amplitude of $h(\nu, \tau_H)$ is reduced by $\sim 10\%$ by the e^+e^- annihilation. Also the frequency range of this reduction covers that of LIGO, VIRGO, LISA, etc.

Fig.7 is an enlarged portion of the spectrum $h(\nu, \eta_H)$ around $\nu = 10^{-9}$ Hz, illustrating the details of reductions of the spectrum by both QCD transition and e^+e^- annihilation. The combination of the QCD transition and the e^+e^- annihilation reduce $h(\nu, \tau_H) \sim 30\%$.

The influence of the dark energy on the spectrum $h(\nu, \tau_H)$ is demonstrated in Fig.8, where $\Omega_\Lambda = 0.0, 0.7,$ and 0.75 are taken respectively. As explained in the last section, over the whole range of frequency ($10^{-19} \sim 10^{10}$) Hz, the amplitude of spectrum is suppressed by the presence of Ω_Λ , but the slope remains the same. In particular, $h(\nu, \tau_H)$ with $\Omega_\Lambda = 0.75$ is reduced by $\sim 45\%$ in comparison with the model $\Omega_\Lambda = 0$. (See Eq.(29))

Figure 9 is a comparison of the LIGO detection with our calculated RGWs with the fixed tensor/scalar ratio $r = 0.22$ and the dark energy $\Omega_\Lambda = 0.75$. The upper smooth curve is from the LIGO H1 Upper limits (95% CL) from PowerFlux best-case [42], and the lower three fluctuating curves are the RGWs spectra of $\beta = -1.8, -1.9,$ and -2.02 , corresponding to those in Fig.3, respectively. Here the vertical axis is the root mean square amplitude per root Hz, which equals to

$$\frac{h(\nu)}{\sqrt{\nu}}. \quad (38)$$

The plot gives only the frequency range ($30 \sim 300$) Hz, on which the LIGO works efficiently. The reductions due to the QCD transition and the e^+e^- annihilation have been incorporated in the curve of

calculated $h(\nu, \tau_H)/\sqrt{\nu}$. Our result shows that there is a gap of about one order of magnitude even for the $\beta = -1.8$ inflationary model. As it currently stands, the possibility for LIGO to detect the RGWs predicted by the $\beta = -1.8$ inflationary model is not high, let alone other models with $\beta < -1.8$. Other two model parameters, i.e., the tensor/scalar ratio r and the dark energy Ω_Λ will substantially influence the height of $h(\nu)$. The five-year WMAP data improve the upper limit on the tensor/scalar ratio $r < 0.43$ (95% CL) for power-law inflationary models and $r < 0.58$ (95% CL) for models with a running index, and give the value of dark energy $\Omega_\Lambda = 0.721 \pm 0.015$ [36]. So if we take the upper limit $r = 0.43$ for power-law models, the height of $h(\nu)$ will increase by $\sim 40\%$ by Eq.(33), and, furthermore, if we take $\Omega_\Lambda = 0.721$, $h(\nu)$ will increase by another $\sim 16\%$ [3]. These together will allow an increase of $h(\nu)$ by a total $\sim 62\%$. Therefore, the current LIGO with greatly enhanced sensitivity [4] will definitely be able to put a constraint on the $\beta = -1.8$ inflationary model. However, it is seen from Fig.9 that the curve for $\beta \simeq -2.02$, supported by the scalar inflation models and the WMAP data [18] [36] [37], is about five orders below the LIGO sensitivity. So we may say that the RGWs generated by scalar inflation models is unlikely to be directly detected by LIGO at the moment.

Figure 10 is a comparison of the LISA sensitivity curve with the spectra from Fig.3 in the lower frequency range ($10^{-7}, 10^0$) Hz that is also covered by the modifications of the QCD transition and the e^+e^- annihilation. Assume that LISA has one year observation time corresponding to frequency bin $\Delta\nu = 3 \times 10^{-18}$ Hz (i.e., one cycle/year) around each frequency. To make a comparison with the sensitivity curve, we need to rescale the spectrum $h(\nu)$ in Eq.(31) into the root mean square spectrum $h(\nu, \Delta\nu)$ in the band $\Delta\nu$ [31] [39],

$$h(\nu, \Delta\nu) = h(\nu) \sqrt{\frac{\Delta\nu}{\nu}}. \quad (39)$$

This r.m.s spectrum can be directly compared with the 1 year integration sensitivity curve that is downloaded from LISA [43]. The plot shows that LISA by its present design will be able to detect the inflationary model of $\beta = -1.8$. If the ratio $r > 0.22$, it is still possible for LISA to detect the model of $\beta = -1.9$. However, LISA is unlikely to be able to directly detect the model of $\beta = -2.02$, as there is a gap of two orders. One may say that, in regards to detection of RGWs, LISA will give a stronger constraint on the RGWs spectrum than LIGO will do.

Figure 11 shows the β -dependence of the spectral energy density $\Omega_g(\nu)$ defined in Eq.(34). Clearly, Ω_g is very sensitive to the inflationary parameter β . A larger β gives a higher Ω_g . The Advanced LIGO [4] will be able to detect RGWs with $\Omega_g h^2 > 10^{-9}$ at $\nu \sim 100$ Hz, and it might impose stronger constraints on other inflationary models. On the other hand, the total energy density Ω_{GW} defined in Eq.(35) has also been used as a constraint on RGWs. Taking the parameters $r = 0.22$, $\Omega_\Lambda = 0.75$, $\beta_s = -0.3$, and $n = 1.634$, we find $\Omega_{GW} = 1.11 \times 10^{-2}$ for the inflationary model of $\beta = -1.8$, which is 3 orders higher than the BBN bound [39] in Eq.(36). So this model is disfavored, unless some other mechanism is introduced to reduce its Ω_{GW} . We also obtain $\Omega_{GW} = 1.97 \times 10^{-8}$ for the model $\beta = -1.9$, and $\Omega_{GW} = 1.41 \times 10^{-14}$ for the model $\beta = -2.02$; both models are safely below the BBN bound in Eq.(36).

Fig.12 shows $\Omega_g(\nu)$ in the $\beta = -2.02$ modified by the QCD transition and e^+e^- annihilation, where the reduction on RGWs is more noticeable. In the range $\nu > 10^{-9}$ Hz the QCD transition alone reduces $\Omega_g(\nu)$ by $\sim 30\%$ and the combination of QCD transition and the e^+e^- annihilation reduces $\Omega_g(\nu)$ by

$\sim 50\%$.

The impact of dark energy on $\Omega_g(\nu)$ for the model $\beta = -2.02$ is plotted in Fig.13. Three values of $\Omega_\Lambda = 0.0, 0.70, 0.75$ are taken. A larger Ω_Λ gives a lower Ω_g . It is seen that the Ω_Λ causes a decrease of the amplitude of Ω_g by a factor of 1.6 over the whole range of frequencies.

ACKNOWLEDGMENT: We are grateful the referees for valuable suggestions. Y.Zhang's research work is supported by the CNSF No.10773009, SRFDP, and CAS.

Appendix A: Modelling of QCD transition and e^+e^- annihilation

The detail of the QCD transition is notoriously complicated and still under study. Here we will only consider the change of the effective degree of freedom, and give a simple working model for the scale factor $a(\tau)$ around the QCD transition lasting a short period. Thus the radiation era can be tentatively divided into the three parts with the scale factor $a(t)$ been listed in Eqs.(4), (5), and (6). After using the continuity conditions of $a(\tau)$ and of $a(\tau)'$ at the two given joining points τ_x and τ_2 , one still needs to determine 3 parameters, τ_q, τ_x, n . Since the QCD transition temperature $T \propto 1/a$ during the radiation era, as soon as T is given, the initial time τ_q of QCD transition is determined, so is the parameter ζ_s . Still n and τ_x need to be fixed in the following.

Around the QCD transition, the contributions from the matter ρ_m and the dark energy ρ_Λ can be neglected. Only the radiation is important, of which the energy density, the pressure, and the entropy density are given by

$$\rho_r(T) = \frac{2\pi^2}{30} g_*(T) T^4, \quad (40)$$

$$p_r(T) = \frac{1}{3} \rho_r(T), \quad (41)$$

$$s(T) = (\rho_r + p_r)/T = \frac{2\pi^2}{45} g_{*s}(T) T^3, \quad (42)$$

respectively, where g_* and g_{*s} denote the effective number of relativistic species contributing to the energy density and entropy, respectively [44]. In an adiabatic universe, the entropy per unit comoving volume is conserved

$$S(T) = s(T)a^3(T) = \text{constant}. \quad (43)$$

From Eqs. (40), (42) and (43), one has

$$\rho_r \propto g_* g_{*s}^{-4/3} a^{-4}. \quad (44)$$

During the QCD transition era, one has $g_* = g_{*s}$ [29, 30]. Therefore, here we will not distinguish the difference between g_* and g_{*s} . Thus, Eq.(44) is reduced to

$$\rho_r \propto g_*^{-1/3} a^{-4}, \quad (45)$$

which is plugged into the Friedmann equation $(\frac{a'}{a^2})^2 = \frac{8\pi G}{3} \rho_r$, yielding

$$(a')^2 \propto g_*^{-1/3}. \quad (46)$$

Table 1: The Values of n and ξ_q for different $\frac{t_x}{t_q}$ (T=190MeV)

t_x/t_q	n	ζ_q
1.3	4.556	1.25
1.5	1.634	1.34
1.8	0.899	1.47
2.0	0.714	1.55

Thus, with the decreasing of g_* across the QCD transition the expansion rate a' in terms of the conformal time increases. As predicted by the Standard Model of particle physics, before the QCD transition, $g_*(\tau_q) = 51.25$ at the time τ_q ; and after the QCD transition, it becomes $g_*(\tau_x) = 17.25$ at the time τ_x [45, 46]. Applying Eq.(46) to Eqs.(4) and (6) yields the ratio

$$\frac{a_f}{a_e} = \left[\frac{g_*(\tau_q)}{g_*(\tau_x)} \right]^{\frac{1}{6}} \simeq 1.2. \quad (47)$$

From the expression $\zeta_q = \frac{a(\tau_x)}{a(\tau_q)}$, one has

$$\zeta_q^{\frac{n}{1+n}} = 1.2. \quad (48)$$

If τ_x is determined (equivalent to giving ζ_q), Eq.(48) will fix the parameter n . Let us determine ζ_q . The form of power-law in Eq.(5) implies $g_* \propto \tau^{-6n}$ during the QCD transition era [30], thus Eq.(45) reduces to

$$\rho \propto \tau^{2n} a^{-4}. \quad (49)$$

In terms of the cosmic time t defined by $dt = ad\tau$, Eq.(5) implies

$$a \propto t^{\frac{1+n}{2+n}}. \quad (50)$$

Therefore, one gets

$$\zeta_q \equiv \frac{a(\tau_x)}{a(\tau_q)} = \left(\frac{t_x}{t_q} \right)^{\frac{1+n}{2+n}}. \quad (51)$$

Once the ratio of t_x/t_q is given, then two parameters n and ζ_q can be fixed from Eqs.(48) and (51) immediately. Ref.[45] gives a value of the ratio $t_x/t_q \sim 2$; Ref.[46] estimated the typical duration of QCD transition to be the order of $\sim 0.1t_q$, i.e., $t_x/t_q \sim 1.1$. For concreteness in actual calculation, we take

$$t_x = (1.3 \sim 2.0)t_q. \quad (52)$$

In Table 1 the values of n and ξ_q are listed for each given value of t_x/t_q . Here our treatment is different from that in Ref.[30], where the choice of n was put in by hand.

In our model, there are three physical parameters: the QCD transition temperature T (i.e. the beginning time t_q), the duration of transition (i.e. the ratio t_x/t_q), and the change of g_* (i.e. the behavior of $a(\tau)$ during the transition). As our calculation shows, $\Omega_g(\nu)$ is not very sensitive to the concrete values of T and of t_x/t_q . For $T = 160$ and 190 Mev, the difference in $\Omega_g(\nu)$ is only $\sim 1\%$, and, similarly, for $t_x/t_q = 1.3$ and 2 the difference in $\Omega_g(\nu)$ is only $\sim 1\%$. This small difference is also reflected by the total

Table 2: Ω_{GW} for different QCD transition models

with QCD transition	$\Omega_{GW}(160MeV)$	$\Omega_{GW}(190MeV)$
$t_x/t_q = 1.3$	1.40×10^{-14}	1.44×10^{-14}
$t_x/t_q = 1.5$	1.38×10^{-14}	1.41×10^{-14}
$t_x/t_q = 2.0$	1.35×10^{-14}	1.36×10^{-14}
without QCD trnsition	1.54×10^{-14}	1.54×10^{-14}

energy density Ω_{GW} for different T and t_x/t_q listed in Table 2 for $r = 0.22$, $\Omega_\Lambda = 0.75$, $\beta = -2.02$, and $\beta_s = -0.3$. Therefore, as a conclusion, the most important element affecting the spectrum of RGWs is the change of g_* , which are completely determined by the Standard Model of particle physics.

The same treatment can be applied to the e^+e^- annihilation. According to the Standard Model of particle physics, before the e^+e^- annihilation, $g_*(\tau_y) = g_{*s}(\tau_y) = 10.75$ at the time τ_y ; and after the e^+e^- annihilation, $g_*(\tau_z) = 3.36$ and $g_{*s}(\tau_z) = 3.91$ at the time τ_z [29, 30]. Applying Eq.(44) to Eqs.(6) and (8) yields the ratio

$$\frac{a_g}{a_f} = \frac{g_*^{-1/2}(\tau_y) g_{*s}^{2/3}(\tau_y)}{g_*^{-1/2}(\tau_z) g_{*s}^{2/3}(\tau_z)} \simeq 1.1. \quad (53)$$

One can obtain

$$\zeta_y^{\frac{v}{1+v}} = 1.1. \quad (54)$$

Since $T \propto 1/a$ and the e^+e^- annihilation occurred during $T \simeq (0.5 \sim 0.1)$ MeV [30], one obtains $\zeta_y \equiv \frac{a(\tau_z)}{a(\tau_y)} = 5$ and $v = 0.063$ that are used in Eq.(7).

Appendix B: Simple interpretation of modifications of RGWs by QCD transition and e^+e^- annihilation

Given the wave equation in Eq.(23), there are two limiting cases for wavelength. For the short wavelength $k \gg \frac{a'}{a}$, the mode function h_k has a decreasing amplitude,

$$h_k(\tau) \propto 1/a(\tau). \quad (55)$$

and, for the long wavelength $k \ll \frac{a'}{a}$, the mode h_k is simply a constant

$$h_k(\tau) \simeq C_k. \quad (56)$$

This property itself will be able to qualitatively account for why the QCD transition induces a decrease in the spectrum $h(\nu, \tau_H)$ in Eq.(37). In Fig.14 the scale factor $a(\tau)$ is plotted for the QCD transition era around $T \sim 190$ Mev, and it is seen that

$$a(\tau)_{QCD} = a(\tau)_{noQCD}, \quad \tau < 10^{-9}, \quad (57)$$

$$\frac{a(\tau)_{QCD}}{a(\tau)_{noQCD}} \simeq 1.2, \quad \tau > 10^{-9}. \quad (58)$$

This result, together with Eq.(55), explains the reduction of $h(\nu, \tau_H)$ by $\sim 20\%$ by the QCD transition, as explicitly shown in Fig.5. We need to explain why the reduction occurs for $\nu > \nu_Q = 10^{-9}$ Hz. Since at any time τ those modes with

$$k > \frac{a'(\tau)}{a(\tau)} \simeq \frac{1}{\tau} \quad (59)$$

will decay as in Eq.(55), one sees that only those modes with

$$k > k_Q \equiv \frac{1}{\tau_q} \quad (60)$$

will be reduced by the QCD transition. According to Eq.(18), in the present universe the physical frequency corresponding to k_Q is

$$\nu_Q = \frac{k_Q}{2\pi a(\tau_H)} = \frac{H_0}{2\pi\gamma\tau_q} \simeq 10^{-9} \text{ Hz} \quad (61)$$

for $\gamma = 1.044$ and the Hubble constant $H_0 \simeq 2.36 \times 10^{-18}$ Hz. This critical frequency ν_Q in Eq.(61) matches that demonstrated in Fig.5 and Fig.12, and is about 2 orders lower than 10^{-7} Hz, a value quoted in Ref. [29]. Thus, the features in the calculated spectrum of RGWs have been fully explained. We remark that a higher temperature T of the QCD transition would yield an earlier time τ_q and a higher critical frequency ν_Q . As for the reduction by e^+e^- annihilation, the interpretation is similar to the above.

References

[*] e-mail: yzh@ustc.edu.cn

- [1] L. P. Grishchuk, Sov.Phys.JETP **40**, 409 (1975); Class.Quant.Grav.**14**, 1445 (1997); astro-ph/0008481.
- [2] A. A. Starobinsky, JEPT Lett. **30** 682 (1979); Sov.Astron.Lett.**11**, 133 (1985); V. A. Rubakov, M.Sazhin, and A. Veryaskin, Phys.Lett.B **115**, 189 (1982); R. Fabbri & M.D. Pollock, Phys.Lett.B**125**, 445 (1983); L. F. Abbott & M.B. Wise, Nucl.Phys.B**244**, 541 (1984); L. F. Abbott & D. D. Harari, Nucl.Phys.B**264**, 487(1986); B. Allen, Phys.Rev.D**37**, 2078 (1988); V. Sahni, Phys.Rev.D**42**, 453 (1990); A. Riazuelo & J. P. Uzan, Phys.Rev.D**62**, 083506 (2000); H. Tashiro, et.al, Class.Quant.Grav.**21**, 1761 (2004); A. B. Henriques, Class.Quant.Grav.**21**, 3057 (2004); L. A. Boyle and P. J. Steinhardt, arXiv:astro-ph/0512014
- [3] Y. Zhang, et.al., Class. Quant. Grav. **22**, 1383 (2005); Chin. Phys. Lett. **22**, 1817 (2005); Class. Quant. Grav.**23**, 3783 (2006).
- [4] <http://www.ligo.caltech.edu/>; <http://www.ligo.caltech.edu/advLIGO>.
- [5] <http://wwwcascina.virgo.infn.it/>.
- [6] <http://www.geo600.uni-hannover.de/>.
- [7] <http://tamago.mtk.nao.ac.jp/>.
- [8] <http://www.anu.edu.au/Physics/ACIGA/>
- [9] <http://lisa.nasa.gov/>; <http://www.lisa.caltech.edu/>
- [10] W.T. Ni, S. Shiomi and A.C. Liao, Class.Quant.Grav. **21** S641 (2004).
- [11] <http://universe.nasa.gov/program/bbo.html>; V. Corbin and N.J. Cornish, Class.Quant.Grav. **23** 2435 (2006).
- [12] N. Seto, S. Kawamura and T. Nakamura, Phys.Rev.Lett. **87** 221103 (2001).
- [13] M.M. Basko & A.G. Polnarev, MNRAS **191**, 207 (1980); A.G. Polnarev, AZh, **62**, 1041 (1985); N. Kaiser, MNRAS **202**, 1169 (1983); J.R. Bond & G. Efstathiou, ApJ **285**, L45 (1984); MNRAS **226**, 655 (1987); R. Crittenden, R.L. Davis, P.J. Steinhardt, ApJ **417**, L13 (1993); R.G. Crittenden, D. Coulson, and N.G. Turok, Phys.Rev.D**52**, R5402 (1995); D. Coulson, R.G. Crittenden, and N.G. Turok, ApJ **417**, L13 (1993); D.D. Harari & M. Zaldarriaga, Phys.Lett.B**319**, 96 (1993); M. Zaldarriaga & D.D. Harari, Phys.Rev.D**52**, 3276 (1995); R.A. Frewin, A.G. Polnarev, P. Coles, MNRAS, 266, L21 (1994). B.G. Keating, P.T. Timbie, A. Polnarev, and J. Steinberger, ApJ, **495**, 580 (1998); A. Kosowsky, Ann.Phys. **246**, 49 (1996); M. Zaldarriaga & U. Seljak, Phys.Rev.D**55**, 1830 (1997); U. Seljak & M. Zaldarriaga, Phys.Rev.Lett.**78**, 2054 (1997) W. Hu & M. White, Phys Rev D**56**, 596 (1997)

- [14] M. Kamionkowski, A. Kosowsky, and A. Stebbins, *Phys.Rev.D***55**, 7368 (1997)
- [15] J. R. Pritchard & M. Kamionkowski, *Annals. Phys.***318**, 2 (2005).
- [16] W. Zhao and Y. Zhang, *Phys.Rev.D***74**, 083006 (2006).
- [17] D. Baskaran, L.P. Grishchuk, and A.G. Polnarev, *Phys. Rev. D***74**, 083008 (2006); Polnarev A.G., Miller N.J., Keating B.G., arXiv: astro-ph 0710.3649.
- [18] D.N. Spergel, et al, *ApJS* **148**, 175 (2003).
D.N. Spergel, et.al. *ApJS* **170**, 377 (2007).
- [19] M. Tegmark et.al. *Phys.Rev. D***74**, 123507 (2006)
- [20] U. Seljak, A. Slosar and P. McDonald, *JCAP* **0610**, 014 (2006).
- [21] L. Page, et.al. *ApJS* **170**, 335 (2007).
- [22] G. Hinshaw et.al. *ApJS* **170**, 263 (2007).
- [23] T. L. Smith, M. Kamionkowski and A. Cooray, *Phys.Rev. D***73**, 023504 (2006); W. Zhao and Y. Zhang, *Phys.Rev.D***74**, 043503 (2006).
- [24] A.G. Riess, *et al.*, *Astron.J.* **116**, 1009 (1998); *ApJ*. **117**, 707 (1999); S. Perlmutter *et al.*, *ApJ* **517**, 565 (1999); J.L. Tonry *et al.*, *ApJ* **594**, 1 (2003); R.A. Knop *et al.*, *ApJ* **598**, 102 (2003); A.G. Riess *et al.*, *Astron.J.* **607**, 665 (2004).
- [25] S. Weinberg, *Phys.Rev.D***69**, 023503 (2004); D. A. Dicus and W. W. Repko, *Phys.Rev.D***72**, 088302 (2005).
- [26] H.X. Miao and Y. Zhang, *Phys.Rev.D***75**, 104009 (2007).
- [27] M. Cheng et al, *Phys.Rev.D***74**, 054507 (2006).
- [28] F. Karsch, arXiv:0711.0661.
- [29] D. J. Schwarz, *Mod.Phys.Lett.A***13**, 2771 (1998).
- [30] Y. Watanabe and E. Komatsu, *Phys.Rev.D***73**, 123515 (2006).
- [31] L. P. Grishchuk, in *Lecture Notes in Physics*, Vol. 562, p.167, Springer-Verlag, (2001), (gr-qc/0002035).
- [32] A.R. Liddle and D.H. Lyth, *Phys.Lett. B***291**, 391 (2006).
- [33] Y. Zhang, *Gen.Rel.Grav.***34**, 2155 (2002); *Gen.Rel.Grav.***35**, 689 (2003); *Chin.Phys.Lett.***20**, 1899 (2003); *Chin.Phys.Lett.***21**, 1183 (2004). W. Zhao and Y. Zhang, *Phys.Lett. B***640**, 69 (2006); *Class.Quant.Grav.***23**, 3405 (2006). Y. Zhang, T.Y. Xia, and W. Zhao, *Class.Quant.Grav.***24**, 3309 (2007). T.Y. Xia and Y. Zhang, *Phys.Lett. B***656**, 19 (2007).
- [34] L. P. Grishchuk, *Phys.Rev.D***48**, 3513 (1993).
- [35] L. Parker, *Phys.Rev.***183**, 1057 (1969).
- [36] J. Dunkley, et al, arXiv:astro-ph 0803.0586.
- [37] G. Hinshaw, et al, arXiv:astro-ph 0803.0732; E. Komatsu, et al, arXiv:astro-ph 0803.0547
- [38] U. Seljak, et.al., *Phys.Rev. D***71** 103515 (2005); A. Cooray, P.S. Corasaniti, T. Giannantonio and A. Melchiorri, *Phys. Rev. D***72**, 023514 (2005); T.L. Smith, M. Kamionkowski and A. Cooray, *Phys. Rev. D***73**, 023504 (2006); arXiv: astro-ph 0802.1530; A. Linde, V. Mukhanov and M. Sasaki, *JCAP* **0510**, 002 (2005); V. Mukhanov and A. Vikman, *JCAP* **0602**, 004 (2006).
- [39] M. Maggiore, *Phys.Rept.***331**, 283 (2000); R.H. Cyburt, J. Ellis, B.D. Fields, and K.A. Olive, *Phys. Rev. D***67**, 103521 (2003); R.H. Cyburt et.al. *Astropart.Phys.***23**, 313 (2005); T.L. Smith, E. Pierpaoli, and M. Kamionkowski, *Phys.Rev.Lett***97**, 021301 (2006).
- [40] F.Y. Li, M.X. Tang, and D.P. Shi, *Phys.Rev.D***67**, 104008 (2003); M.L. Tong, Y. Zhang, and F.Y. Li, under preparation.
- [41] A.M. Cruise, *Class.Quant.Grav.* **17**, 2525 (2000) ; A.M. Cruise and R.M.J. Ingle, *Class.Quant.Grav.***22**, S479 (2005); *Class.Quant.Grav.***23**, 6185 (2006). M.L. Tong and Y. Zhang, arXiv:gr-qc 0711.4909, to appear in *ChJAA* (2008).
- [42] B. Abbott, et al. 2007 arXiv:0708.3818
- [43] <http://www.srl.caltech.edu/~shane/sensitivity>.
- [44] E.W. Kolb and M. S. Turner, *The Early Universe* (Addison-Wesley, Reading, MA, 1990).
- [45] B. Kampfer, *Ann.Phys.* **9**, 605 (2000).
- [46] D.J. Schwarz, *Ann.Phys.* **12**, 220 (2003); D. Boyanovsky, H.J. de Vega, and D.J. Schwarz, *Ann. Rev. Nucl. Part. Sci.* **56**, 441, (2006).

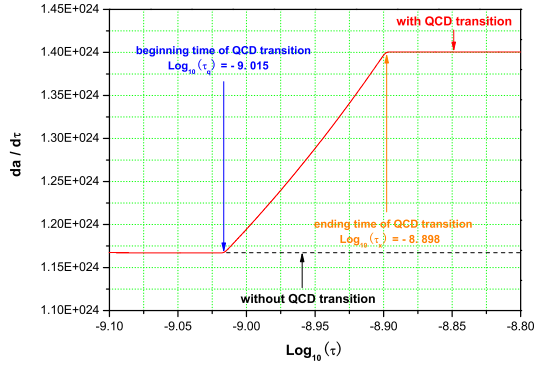


Figure 1: The derivative $a'(\tau)$ jumps up around the QCD transition modelled by Eq.(5). If there were no QCD transition, $a'(\tau)$ would be a constant in this graph.

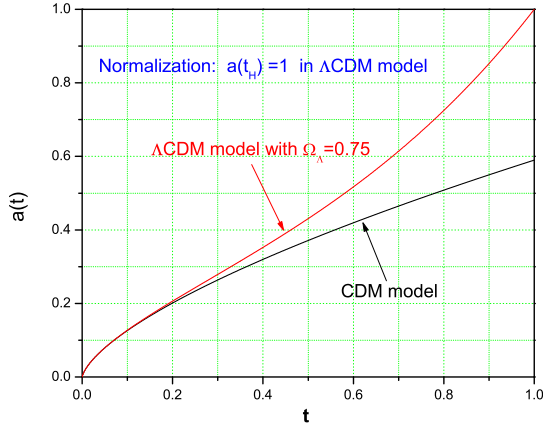


Figure 2: The scale factor $a(t)$ in the accelerating, and non-accelerating models, respectively. Note that the horizontal axis is the cosmic time t . At the present time $t = 1$ the ratio of scale factors is $a_{\Lambda\text{CDM}}/a_{\text{CDM}} \simeq 1.8$.

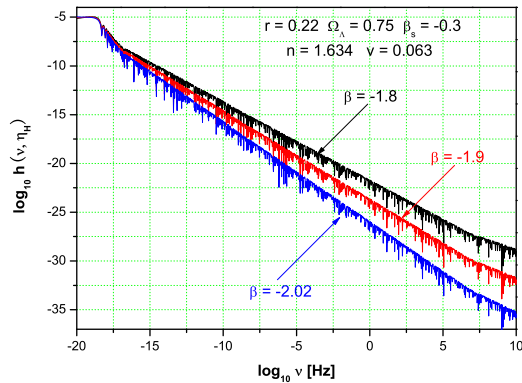


Figure 3: The spectrum $h(\nu, \tau_H)$ of GRWs is very sensitive to the index β of inflation.

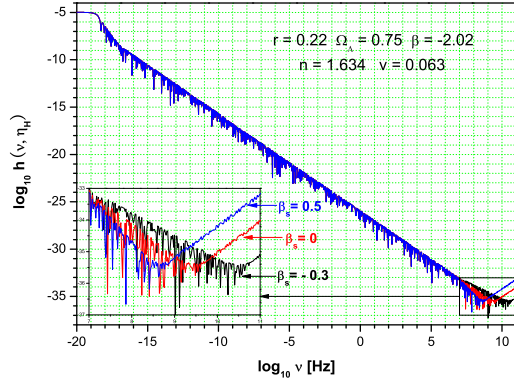


Figure 4: The reheating affects the spectrum $h(\nu, \tau_H)$ only in very high frequency range $\nu > 10^7$ Hz.

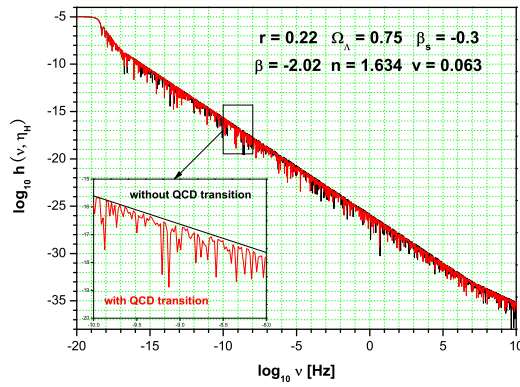


Figure 5: The QCD transition reduces $h(\nu, \tau_H)$ by $\sim 20\%$ in the high frequency range $\nu > 10^{-9}$ Hz, which covers the frequency band of LIGO and LISA.

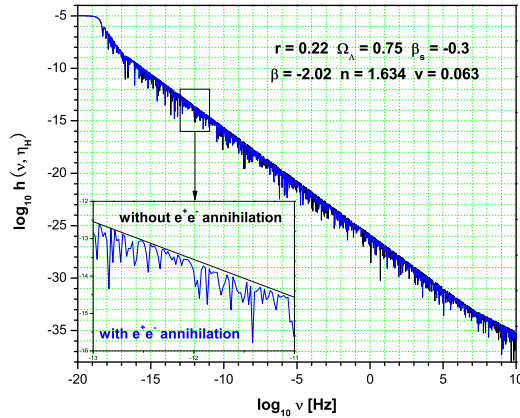


Figure 6: The e^+e^- annihilation reduces $h(\nu, \tau_H)$ by $\sim 10\%$ in the frequency range $\nu > 10^{-12}$ Hz, which covers the frequency band of LIGO and LISA.

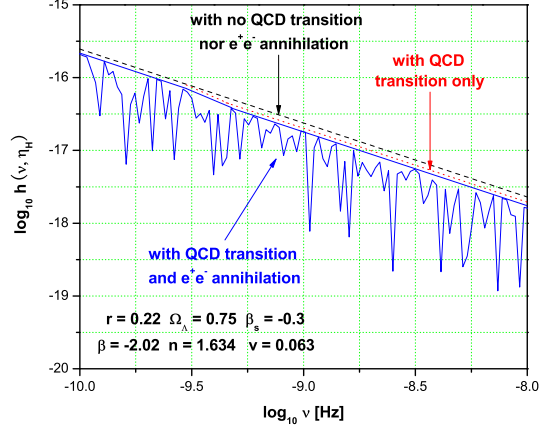


Figure 7: The spectrum $h(\nu, \tau_H)$ around $\nu = 10^{-9}$ Hz for three cases: (1) with no QCD transition nor e^+e^- annihilation, (2) with QCD transition only, (3) with both QCD transition and e^+e^- annihilation.

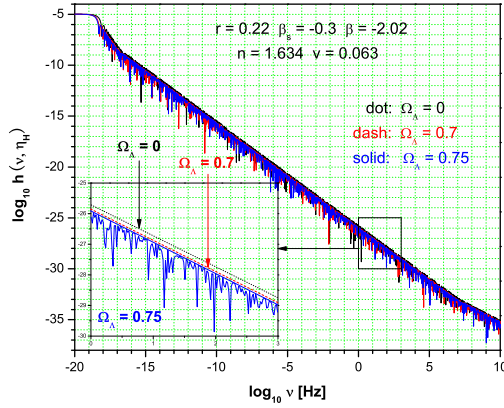


Figure 8: The spectrum $h(\nu, \tau_H)$ depends upon the dark energy Ω_Λ in the accelerating universe. A larger Ω_Λ yields a lower $h(\nu, \tau_H)$.

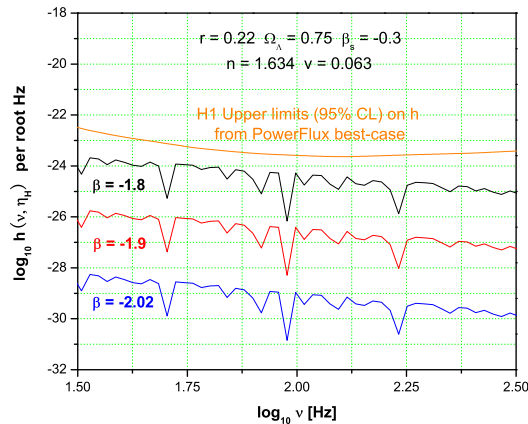


Figure 9: Comparison of the spectra with the LIGO H1 Upper limits (95% CL) from PowerFlux best-case in the Ref.[42]. The vertical axis is the r.m.s amplitude per root Hz defined in Eq.(38).

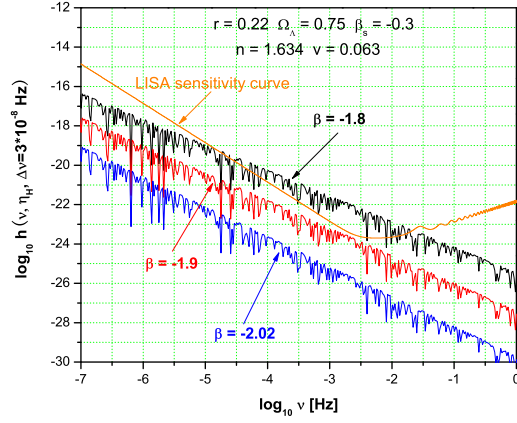


Figure 10: Comparison of the spectra with the LISA sensitivity curve [43]. The vertical axis is the r.m.s spectrum defined in Eq.(39). The inflationary model of $\beta = -1.8$ can be tested by the LISA.

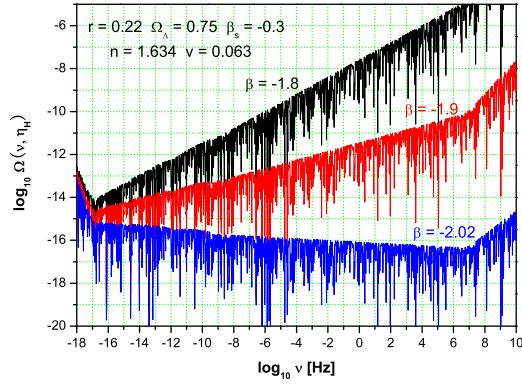


Figure 11: The spectral energy density $\Omega_g(\nu)$ for various values of the parameter β .

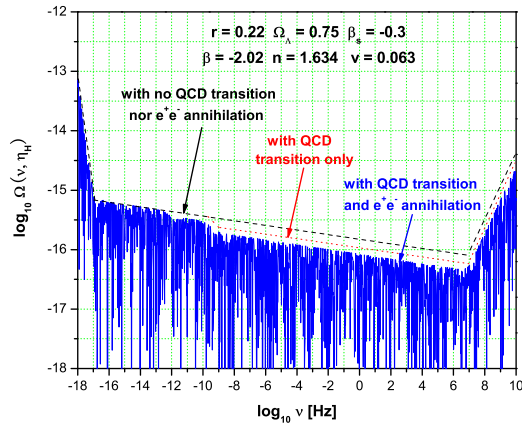


Figure 12: The spectral energy density $\Omega_g(\nu)$ for three cases: (1) with no QCD transition nor e^+e^- annihilation, (2) with QCD transition only, (3) with both QCD transition and e^+e^- annihilation.

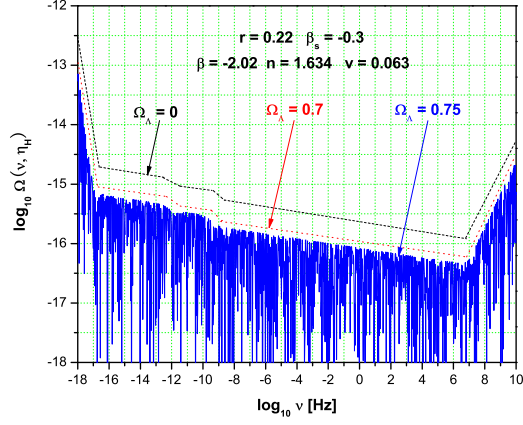


Figure 13: The spectral energy density $\Omega_g(\nu)$ for different Ω_Λ . A larger Ω_Λ yields a lower $\Omega_g(\nu)$.

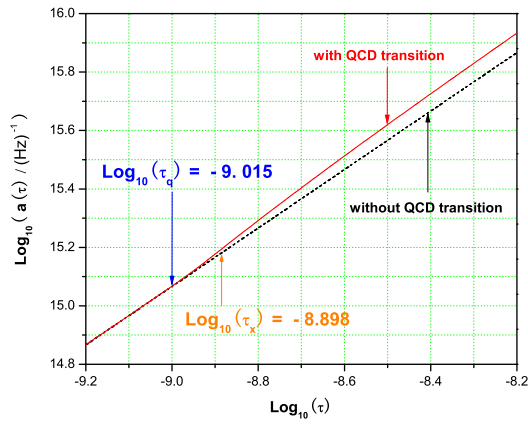


Figure 14: The scale factor $a(\tau)$ is affected by the QCD transition. For $\tau < 10^{-9}$, $a(\tau)_{QCD} = a(\tau)_{noQCD}$. But for $\tau > 10^{-9}$, $a(\tau_H)_{QCD}/a(\tau_H)_{noQCD} \simeq 1.2$.